PHYSICAL REVIEW A, VOLUME 61, 011404(R)

Ultracold collisions in saturating optical fields: Universal behavior in the entrance channel

James P. Shaffer,[1,2] Witek Chalupczak,[2] and N. P. Bigelow[2]
[1]*The Institute of Optics, The University of Rochester, Rochester, New York, 14627*
[2]*Department of Physics and Astronomy and The Laboratory for Laser Energetics, The University of Rochester, Rochester, New York, 14627*

(Received 16 March 1999; published 8 December 1999)

We present precise near-dissociation limit measurements of ultracold collision rate constants (trap loss, fine-structure changing, and photoassociative ionization) as a function of trap intensity from I_{sat} to $I \approx 40 I_{sat}$ for Cs and Na atoms cooled and confined in a magneto-optical trap. We find strong saturation for all processes at intensities approximately 10 times the free atom saturation level I_{sat}. Our results provide a precise reference point for testing and comparing different theoretical models used to analyze ultracold collisions.

PACS number(s): 32.80.Pj, 03.75.Fi, 05.30.Jp

The investigation of optically activated collisions between atoms in the magneto-optical trap (MOT) has attracted a great deal of interest in recent years [1]. A rich array of phenomena has been investigated, including the photoassociation of atoms into long-range molecular states [2], the controlled formation of molecular ions [3] [photoassociative ionization (PAI)], and the observation of hyperfine [1] and fine-structure (FS) changing collisions [4]. One important unifying feature is that all of these collisions share a common entrance channel in which a colliding ground-state atomic pair absorbs a photon at long range (outside the LeRoy distance [5]). This photoassociation event results in the creation of an excited molecule — a key precursor to trap loss. A great deal is understood about these photoassisted collision processes [1]. Nevertheless, the picture remains incomplete, and it is still not possible to predict what the collisional trap loss rate will be for a given set of trap laser parameters such as detuning and intensity.

The theoretical treatment of the intensity dependence of the collisional loss rate in the MOT is a complicated yet intriguing problem in part because spontaneous emission and hence dissipation play a leading role. Recently, significant progress has been made in developing techniques for treating intensity-dependent collision rates [6] and, as a result, there is an increasing need for experimental data to compare with theoretical models.

In this paper we present data on the intensity dependence of four different trap-loss studies, examining two different atomic species (Na and Cs), each trapped in a MOT [7]. We find that within each species, clear saturation of different rates is observed, and that the saturation shows remarkably universal behavior. In particular, we find that (1) all rates saturate at an intensity well above the bare atom saturation intensity, (2) that this saturation occurs in an identical manner in Cs for the overall trap loss rate and for the fine-structure changing collision rate, and (3) that in Na saturation occurs in an identical manner for the overall trap loss rate and for the photoassociative ionization rate. We then characterize our data using a two-state model for the entrance channel. To date, such clear saturation has not to our knowledge, been experimentally reported [8,9].

The systems under study are laser-cooled vapors of Cs and Na atoms contained in a MOT. The trapping laser beams for the Na and Cs MOTs are frequency referenced to saturated absorption spectrometers. To operate the Na trap the laser is detuned, $\Delta = -13$ MHz, from the $3\,^2S_{1/2}(F=2) \rightarrow 3^2P_{3/2}(F'=3)$ D_2 transition. Before being sent to the trap, the 589-nm light is passed through an electrooptic modulator that introduces sidebands shifted from the input laser frequency by ± 1.71 GHz. The blue-detuned sideband couples to the $F=1 \rightarrow F'=2$ Na transition, preventing optical pumping. The intensity of each sideband is 10% of the total intensity. The ratio of populations in the Na ground-state hyperfine states is approximately constant throughout the range of the experiment, $F2/F1 \approx 2.7-4.2$ [10]. The 852-nm light is detuned, $\Delta_{Cs} = -23$ MHz, from the $6\,^2S_{1/2}(F=4) \rightarrow 6\,^2P_{3/2}(F'=5)$ D_2 transition. Cs repumping light is provided by a separate grating stabilized diode laser tuned to the $F=3 \rightarrow F'=4$ transition and has a constant intensity of 1.5 mW/cm^2. The ratio of populations in the ground-state hyperfine states ranges from $[F=4/F=3]=2-32$ [10], changing almost linearly with intensity above ~ 25 mW/cm^2. Both the 589-nm and 852-nm light is relayed to the respective trap through single-mode optical fibers that serve as spatial filters and assure uniform and stable trap beam intensity profiles. Steady-state trapped atoms densities were typically $\sim 10^{10}$ cm^{-3} with $\sim 10^7$ Cs atoms and $\sim 10^6$ Na atoms. All the beams are collimated to 1.5 cm $1/e$ widths. Anti-Helmholtz coils produce a field gradient of 20 G/cm. The chamber is maintained at 10^{-10} Torr, set by the atomic vapor effusing from the source [10,11].

To determine the number of trapped atoms the fluorescence was collected and detected with a calibrated photomultiplier tube (PMT). Careful attention was paid to make sure that the PMT did not saturate. The trap sizes where measured with two charge-coupled-device cameras (spatial resolution <30 μm). Laser intensity was measured with a calibrated power meter. The number of trapped atoms, the trap volume, the atom density, and the rates for FS, PAI, and trap-loss processes were all consistent with previous measurements [1,3,4,10].

The PAI ion rate for the Na MOT was measured by detecting ions produced by the trap using a channel electron multiplier (CEM) ~ 3 cm from the trap. The CEM background count rate was <15 Hz. Using an ion pressure gauge as an alternate source of ions, we determined that the satu-

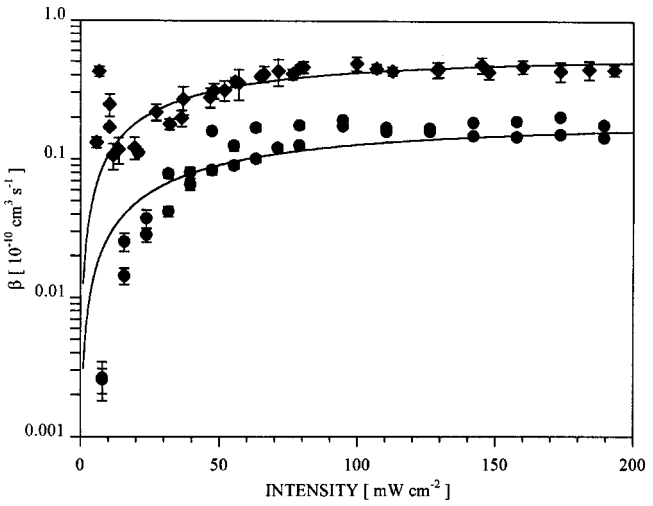

FIG. 1. $\beta_{\mathrm{Na}}(I)$ and $K_{\mathrm{PAI}}(I)$ of the Na trap for the trapping parameters described in the text. Note the axis break. For each value of I approximately 30 measurements were made. The error bars reflect the mean-squared error of the measurement. The solid lines show the fit to the equation described in the text. The circles are β_{Na} while triangles are K_{PAI}.

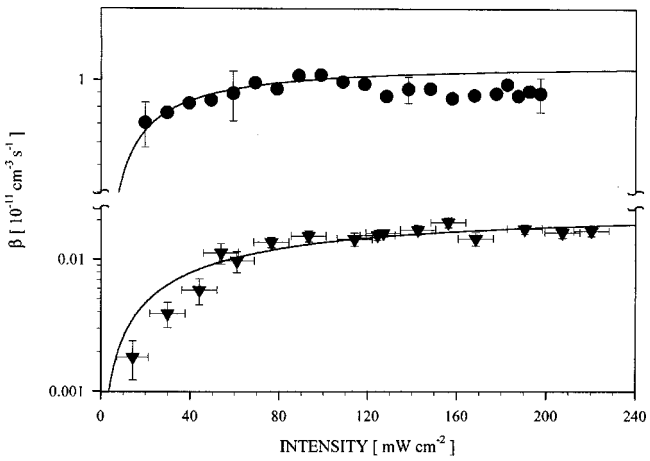

FIG. 2. $\beta_{\mathrm{Cs}}(I)$ and $\beta_{\mathrm{FS}}(I)$ of the Cs trap for the trapping parameters described in the text. Note the axis break. For each value of I approximately 30 measurements were made. The error bars reflect the mean-squared error of the measurement. The solid lines show the fit to the data described in the text. Diamonds are β_{Cs}, while circles are β_{CsFS}. The increase of β_{Cs} at low I is attributed to hyperfine-changing collision [1]. Deviations of β_{CsFS} at low I may be due to uncertainties in trap laser intensity profiles.

ration count rate for the CEM and electronics was more than four orders of magnitude greater than the saturated ion count rate due to collisions in the Na trap. The PAI rate was determined from the measured ion rate and the trapped atom density.

The overall trap-loss rate was measured by monitoring the fluorescence as atoms filled the MOT. We described the filling in terms of the rate equation $dN_i(t)/dt = L - \alpha N_i(t) - \beta N_i^2(t)/V$, which is in the form of the Ricatti equation with constant coefficients. L is the trap loading rate, α is the loss rate due to collisions between ultracold trapped atoms and background atoms, β is the loss rate due to collisions between ultracold trapped atoms, and V is the trap volume. By fitting trap filling curves to this rate equation, β was determined [1,10]

Direct measurement of the Cs FS rate was made by collimating the trap fluorescence and sending it through a 10-nm bandwidth filter selecting $6\,^2S_{1/2} \rightarrow 6\,^2P_{1/2}$ (894-nm) Cs emission. The light then passed through a SPEX 1700-2 1-m monochromator adjusted for an 8-Å bandpass. This eliminated photons from the wing of the $6\,^2S_{1/2} \rightarrow 6\,^2P_{3/2}$ (852-nm) trapping transition. The photons passing through the system were detected by an avalanche photodiode (dark counts <100 Hz). The product of the measured monochromator throughput and the quantum efficiency of the detector was 0.104 and the total throughput (including geometrical factors) was measured to be 2.6×10^{-3}. The filter transmission coefficient was measured as 3.52×10^{-7} at 852 nm and 0.500 at 894. Maximum FS photon count rates were ~ 40 Hz.

Figure 1 shows the trap-loss rate $\beta_{\mathrm{Na}}(I)$ and the PAI rate $K_{\mathrm{Na\text{-}PAI}}(I)$, while Fig. 2 shows the trap-loss rate $\beta_{\mathrm{Cs}}(I)$ and the Cs FS rate $\beta_{\mathrm{Cs\text{-}FS}}\ (I)$. Intensity saturation clearly occurs above the free-atom saturation intensity I_{sat} (6.25 mW/cm^2 for Na and 1.1 mW/cm^2 for Cs). Because different loss processes rely on fundamentally different pathways (e.g., PAI requires the absorption of a second photon at closer range while FS does not), we deduce that the saturation is due to saturation of the common entrance channel. This interpretation is based on the standard picture of optically activated ultracold collisions [12] wherein the first step — photoassociation—takes place at long range (excitation from the ground-ground potential $\sim C_6/R^6$ onto a ground-excited potential $\sim C_3/R^3$) and is followed either by radiative decay or by evolution to short range where the system may undergo a reactive event leading to trap loss.

Experimental data on saturation behavior of the intensity-dependent collision rates in the MOT are limited [1,8,9]. Most relevant to the present work are previous measurements of $K_{\mathrm{PAI}}(I)$ [9] that were used to compare two distinct theoretical techniques. The conclusion of this paper is that calculations based on diabatic solutions of the optical Bloch equations (DOBE) [13] predict a $K_{\mathrm{PAI}}(I)$ closer to the data than calculations using a local equilibrium (LE) [12,14] model (treating spontaneous decay semiclassically and allowing for nonresonant excitation). Although an overall increase of $K_{\mathrm{PAI}}(I)$ with increasing I was reported [9], there was no definitive saturation. More recently, additional models have appeared: one based on a Monte Carlo wave-function [15] method, another based on an alternative adiabatic formulation of the optical Bloch equations [16], and a third based on a delayed-decay Landau-Zener approach [6]. These formulations inspire higher confidence than either the DOBE or LE approaches [6,17] and have led to the conclusion that the excited-state flux in the input channel should not saturate as $I \rightarrow I_{\mathrm{sat}}$, and, indeed, the clear saturation in our measured trap loss, FS, and the PAI rates at $I \gg I_{\mathrm{sat}}$ is consistent with these predictions [6,16].

In the present work, we choose to characterize our data using a two-state model [12,14] for the entrance channel,

TABLE I. Nonradiative rates. The values were obtained by fitting the model described in the text. RE stands for radiative escape; FS stands for fine-structure changing collision. The error listed in the table is the error in the fit. The dominant couplings for the Hund's case (*c*) states as determined in [30] are hyperfine for 0_u^+ to 1_g and for 1_g to 2_u, Coriolis for 0_g^- to 1_g, and quadrupole hyperfine (small) for 0_g^- to 2_u.

Process	Primary zero-order channels	Ref.	Γ (MHz)
β_{Na}	$0_u^+, 1_g, 0_g^-, 1_u$(RE—5%), 2_u(FS—94%)	[12]	78 ± 3
K_{PAI}	0_g	[30]	100 ± 10
β_{Cs}	$0_u^+, 1_g, 0_g^-, 1_u$(RE—67%), 0_u^+(FS—33%)	[4]	81 ± 4
β_{FSCs}	0_u^+, (98%), 2_u(2%)	[12]	95 ± 1

focusing on the role of nonradiative relaxation. We first argue that our situation can be treated within a statistical limit such that we can justifiably treat this complex, multichannel problem using a few-level model. Using this framework, we estimate decay rates for the relevant channels and characterize our data using one parameter: a ''nonradiative'' decay rate.

The reaction rate through an isolated level is $K_P = (hQ_T)^{-1}\Sigma_{l=0}^{\infty}(2l+1)\int_0^{\infty}|S_p(\varepsilon,l,\omega)|^2 e^{-\varepsilon/k_BT}d\varepsilon$, where $Q_T=(2\pi\mu k_BT/h^2)^{3/2}$. ε is the kinetic energy of the atoms, μ is the reduced mass, l is the relative angular momentum of the colliding atomic pair, and $S_p(\varepsilon,l,\omega)$ is the S-matrix element that leads to the formation of product p. A resonant scattering expression for $|S_p(\varepsilon,l,\omega)|^2=\Gamma_p\Gamma_s(\varepsilon,l)/[\Delta^2+(\Gamma/2)^2]$ has been shown to be a reasonable approximation at MOT temperatures [18]. Here $\Gamma=\Gamma_p+\Gamma_s+\Gamma_r+\Gamma_{nr}$. Γ_p is the rate of product formation, $\Gamma_s(\varepsilon,l)$ is the rate of stimulated emission, Γ_r is the spontaneous-emission rate, Γ_{nr} is the rate of nonradiative decay to stable or nonradiating states and to other undetected processes, and Δ is the detuning relative to the bound-state resonance energy. The intensity-dependent expression $|S_p(\varepsilon,l,\omega)|^2$ is used to fit our data. Using release and recapture techniques we have found that our sample remains close to the Doppler temperature T_D over our entire intensity range. We therefore set $T=T_D$ for our fit. For $I\leqslant I_{sat}$, sub-Doppler cooling can be important, but is not relevant here.

As a natural starting point we consider the Hund's case (*c*) states of the collision partners as our basis. There are five attractive electronic basis states for a diatomic alkali-metal molecule that correlate to the $n\,^2S_{1/2}+n\,^2P_{3/2}$ asymptote: 0_g^-, 1_u, 0_u^+, 1_g, and 2_u. It is known that because of interstate couplings, due to first- and second-order Coriolis effects, centrifugal distortion [19], and hyperfine interactions [20], at long-range these states are not exact [21]. More elaborate bases have been computed that are eigenstates of the total angular momentum, energy, and parity [20]; however, nonadiabatic interactions can still mix the states in these bases, such that they too are not exact. In our experiments, photoassociation is via absorption of a MOT photon. Because the MOT laser detuning $\Delta\sim-2\Gamma_{at}$, the absorption occurs near the dissociation limit of the colliding pair. In this case, in the intermediate state there are many levels within one atomic linewidth Γ_{at} [22], and, indeed, experiments on the detuning dependence of the trap-loss rates near the dissociation limit show broad featureless lines [23,24] indicative of this dense, highly coupled level structure.

Given this situation — large interstate and intrastate couplings, combined with a high density of states — we treat the problem in the statistical limit [25]. Here the excited state ψ_n is describable by a superposition of our Hund's case (*c*) basis states, $\psi_n=\Sigma_i\Sigma_j a_{(ij)n}\varphi_{ij}^c+\Sigma_k\Sigma_m a_{(kl)n}\varphi_{km}^c$, where here φ_{ij}^c is an optically active (OA) case (*c*) rovibrational level j of the electronic state i, φ_{km}^c is an optically inactive (OI) case (*c*) rovibrational level m of electronic state k, and the a's are the amplitudes. The $a_{(ij)n}$ largely reflect the allowed excitation of the intermediate states (defining them as OA) but also include the possibility of nonradiative interstate and intrastate couplings between OA states. The $a_{(km)n}$ reflect the coupling of the OI states to the OA states. As long as the OA and OI states do not radiate to any common set of levels, the radiative decay rate of state ψ_n can then be approximated by $\Gamma_n=\Sigma_i\Sigma_j|a_{(ij)n}|^2\Gamma_{ij}+\Sigma_k\Sigma_l|a_{(kl)n}|^2\Gamma_{kl}$ [26]. Assuming that the interstate couplings between OA states is large compared to the inverse of the energy spacing, we may average Γ_{ij} and Γ_{kl} over OA states [27]. $\Gamma_n=\Gamma_r^{\mathrm{av}}+\Gamma_{\mathrm{nr}}^{\mathrm{av}}$. Γ_r^{av} is the OA state averaged coupling to the ground state and $\Gamma_{\mathrm{nr}}^{\mathrm{av}}$ is the average coupling of the OA states to the OI states. In this way we use a two-state model with nonradiative couplings to OI states and adopt the expression $|S_p(\varepsilon,l,\omega)|^2$ to describe our data.

Considering the relevant relaxation rates: $\Gamma_p\sim$ (vibrational frequency) (probability of conversion to product) $=\omega_bP_P\sim(1\mathrm{MHz})(0.01)=0.01$ MHz. There are four zero-order OA electronic states (0_g^-, 1_u, 0_u^+, and 1_g) and one OI electronic state (2_u): $\Gamma_r=2\Gamma_{\mathrm{at}}$, $0.54\Gamma_{\mathrm{at}}$, $1.33\Gamma_{\mathrm{at}}$, $1.21\Gamma_{\mathrm{at}}$ for the 0_g^-, 1_u, 0_u^+, and 1_g attractive states, respectively, while to first order the 2_u state exhibits no dipole relaxation. Γ_{nr} in this picture could only be due to near dissociation couplings to the 2_u rovibrational states. Repulsive Hund's case (*c*) states could also be coupled to the OA electronic states, but the coupling matrix elements will be proportional to small Franck-Condon factors between the coupled levels [28]. So $\Gamma_r^{\mathrm{av}}\approx(2+0.54+1.33+1.21)\Gamma_{\mathrm{at}}/4=1.27\Gamma_{\mathrm{at}}$ (here $\Gamma_{\mathrm{at}}=10$ MHz for Na and 6 MHz for Cs). Using Γ_r^{av} as the spontaneous decay rate in evaluating $|S_p(\varepsilon,l,\omega)|^2$, we fit our data to the form $\frac{1}{2}[I/I_{\mathrm{sat}}]/[1+I/I_{\mathrm{sat}}+(\Gamma_{\mathrm{nr}}^{\mathrm{av}}/\Gamma_r^{\mathrm{av}})^2]$. Here, because the bound-state structure is dense, we use $\Delta\sim0$. These fits are shown as solid lines in Figs. 1 and 2. Resulting values of $\Gamma_{\mathrm{nr}}^{\mathrm{av}}$, the rate of coupling of the OA states to the near dissociation OI 2_u states, are given in Table I. Notice that for a given species, the values of Γ_{nr} are equivalent to within Γ_r.

In conclusion we have demonstrated a universal behavior in the intensity dependence of ultracold collision rates in the MOT. Our data provide a unique reference point for evaluating different trap-loss models. We characterized our data using a two-state model heuristically justified in terms of intrastate and interstate couplings near the $n\,^2S_{1/2}+n\,^2P_{3/2}$ dissociation limit. The saturation that we have observed indicates larger decay rates than in the free-atom case, and in our model this is attributed to coupling of OI to OA states. Our treatment suggests that approaches based on a RRKM-type statistical theory [29] may be a key to understanding the intensity dependence of trap-loss rates. However, our conclusion requires further examination, and the detailed interpretation of the extracted decay rate remains an open challenge.

This work was supported by the National Science Foundation and the David and Lucille Packard Foundation. J.P.S. thanks the Horton Foundation. We thank E. Arimondo and A. Fioretti for valuable discussions.

[1] J. Weiner, Adv. At., Mol., Opt. Phys. **35**, 45 (1995); J. Weiner *et al.*, Rev. Mod. Phys. **71**, 1 (1999), and references therein.

[2] H. Wang *et al.*, Z. Phys. D: At., Mol. Clusters **36**, 317 (1996); P. D. Lett *et al.*, Ann. Rev. Phys. Chem. **46**, 423 (1995), and references therein.

[3] P. D. Lett *et al.*, Phys. Rev. Lett. **67**, 2139 (1991); P. D. Lett *et al.*, *ibid.* **71**, 2200 (1993).

[4] A. Fioretti *et al.*, Phys. Rev. A **55**, R3999 (1997). We note that these measurements indicate saturation in the FS changing rate and that these data are in excellent agreement with our results.

[5] R. J. LeRoy, in *Molecular Spectroscopy 1*, edited by R. F. Borrow, D. A. Long, and D. J. Miller (Chemical Society, London, 1973), pp. 113–176.

[6] K.-A. Suominen *et al.*, Phys. Rev. A **57**, 3724 (1998).

[7] E. L. Raab *et al.*, Phys. Rev. Lett. **59**, 2631 (1987).

[8] L. Marcassa *et al.*, Phys. Rev. A **47**, R4563 (1993); S.-Q. Shang *et al.*, *ibid.* **50**, R4449 (1994); L. Marcassa *et al.*, J. Phys. B **29**, 3051 (1996).

[9] V. S. Bagnato *et al.*, Phys. Rev. A **48**, R2523 (1993).

[10] J. P. Shaffer *et al.*, Appl. Phys. B (to be published). In this paper we show that our traps are best described using a constant-volume approximation and that the difference between constant-volume and constant-density assumptions in trap-filling analysis gives less than a 20% shift in extraction of cold-collision trap-loss rate coefficients.

[11] A. Cable *et al.*, Opt. Lett. **15**, 507 (1990).

[12] P. Julienne and J. Vigue, Phys. Rev. A **44**, 4464 (1991).

[13] Y. B. Band and P. S. Julienne, Phys. Rev. A **46**, 330 (1992).

[14] A. Gallagher and D. E. Pritchard, Phys. Rev. Lett. **63**, 957 (1989).

[15] M. J. Holland *et al.*, Phys. Rev. Lett. **72**, 2367 (1994).

[16] P. S. Julienne *et al.*, Phys. Rev. A **49**, 3890 (1994).

[17] Y. B. Band *et al.*, Phys. Rev. A **50**, R2826 (1994).

[18] R. Napolitano *et al.*, Phys. Rev. Lett. **73**, 1352 (1994).

[19] L. Veseth, J. Phys. B **5**, 1473 (1973).

[20] C. J. Williams and P. S. Julienne, J. Chem. Phys. **101**, 2634 (1994); C. J. Williams *et al.*, Phys. Rev. A **53**, R1939 (1996); E. Tiesinga *et al.*, *ibid.* **57**, 4257 (1998); E. Tiesinga *et al.*, *ibid.* **57**, 4257 (1998).

[21] Since the vibrational levels are nearly degenerate, Fermi-type resonances may also cause both intrastate and interstate couplings.

[22] The number of levels per unit frequency

$$dG(\nu)/d\nu=[\sqrt{2\pi/\mu}3\hbar\Gamma(4/3)/[\Gamma(5/6)C_3^{1/3}]^{-6}(\nu_D-\nu)^{-5/2} \gg\Gamma_{\mathrm{at}}^{-1},$$

where Γ_{at} is the free atom spontaneous decay rate, $\Gamma(n)$ is the gamma function, ν is the vibrational quantum number, ν_D is the vibrational quantum number at the dissociation limit, and μ is the reduced mass [see R. J. LeRoy, Can. J. Phys. **50**, 953 (1972); R. J. LeRoy and M. G. Barwell, *ibid.* **53**, 1983 (1975)].

[23] M. G. Peters *et al.*, Phys. Rev. A **50**, R906 (1994); D. Hoffman *et al.*, Phys. Rev. Lett. **69**, 753 (1992); P. Feng *et al.*, Phys. Rev. A **47**, R3495 (1993); P. Lett *et al.*, J. Phys. B **28**, 65 (1995); D. Sesko *et al.*, Phys. Rev. Lett. **63**, 961 (1989).

[24] K.-A. Suominen *et al.*, Phys. Rev. A **51**, 1446 (1995); K.-A. Suominen *et al.*, *ibid.* **53**, 1678 (1996).

[25] J. Jortner and R. Levine, Adv. Chem. Phys. **47**, 1 (1981).

[26] T. Uzer, Phys. Rep. **199**, 73 (1991).

[27] Here we assume a geometrical average.

[28] Overlap of the wave functions occurs in regions where the wave functions oscillate rapidly, giving rise to small Frank-Condon factors.

[29] W. H. Miller, J. Phys. Chem. A **102**, 793 (1998).

[30] R. W. Heather and P. S. Julienne, Phys. Rev. A **47**, 1887 (1993).